Journal of Hazardous Materials 185 (2011) 662–668

Contents lists available at ScienceDirect

Journal of Hazardous Materials

journal homepage: www.elsevier.com/locate/jhazmat

Leaching of metals from fresh and sintered red mud

Indrani Ghosh[a,*], Saumyen Guha[a], R. Balasubramaniam[b,1], A.V. Ramesh Kumar[c]

[a] Department of Civil Engineering, Indian Institute of Technology, Kanpur 208016, India
[b] Department of Materials and Metallurgical Engineering, Indian Institute of Technology, Kanpur 208016, India
[c] Electrochemistry and Corrosion Division, Defence Materials and Stores Research and Development Establishment, Kanpur 208013, India

ARTICLE INFO

Article history:
Received 5 June 2010
Received in revised form 3 September 2010
Accepted 19 September 2010
Available online 29 September 2010

Keywords:
Red mud
Sintering
Pollution potential
Leachability
Sequential extraction

ABSTRACT

The disposal of red mud, a solid waste generated during the extraction of alumina from bauxite, is one of the major problems faced by the aluminum industry. Proper disposal followed by its utilization, for example as bricks, can provide a satisfactory solution to this problem. Pollution potential of red mud and its finished product, due to metals leaching out from them under certain environmental conditions, need to be studied. Sintering of red mud was performed in a resistance type vertical tube furnace to simulate the brick-making conditions in lab-scale. Leachability of metals in red mud and the sintered product was evaluated by performing sequential extraction experiments on both. The metals studied were the 'macro metals' iron and aluminum and the 'trace metals' copper and chromium. The total extractabilities of all the metals estimated by the microwave digestion of red mud samples decreased due to sintering. The leachability in sequential extraction of the macro metals iron and aluminum, on the other hand, increased due to sintering in all phases of sequential extraction. However, the effect of sintering on the leachability of the trace metals by sequential extraction was different for copper and chromium in different fractions of sequential extraction.

1. Introduction

Every ton of raw bauxite processing leads to approximately 0.5 metric ton of waste red mud and yields approximately 0.5 metric ton of alumina which gives the final end product of about 0.25 metric ton of aluminum [1]. The red mud is highly alkaline and consists of a number of metals that can adversely affect the environment if not contained properly. The cost of disposal of red mud contributes a significant portion to the cost of the product.

Conventionally, red mud slurry is pumped into clay-lined dams or dykes [2] and allowed to dry naturally. Conventional disposal systems were inexpensive, but the potential impact on surrounding groundwater and environment, and difficulties associated with surface rehabilitation, forced significant changes in the disposal practices [1]. Doubly sealed impoundments incorporating a polymeric membrane as well as clay lining, and drained lakes with a drainage network incorporated in the lining material, have been used in recent times [2]. Drained disposal systems reduce the threat of the residue to the environment, increase storage capacity as a result of better residue consolidation and reduce the overall disposal costs.

Concentration of heavy metals such as cadmium, copper, nickel and zinc in red mud are 2–3 orders of magnitude more than the National Oceanographic and Atmospheric Administration (NOAA) Sediment Quality Guidelines [3]. Studies had reported the potential toxicity of red mud to sediment associated biota [4]. Sequential extractions of trace metals from fresh red mud provided information about their mode of occurrence and potential for mobilization under varying physico-chemical and biological conditions [5,6]. Use of dewatered red mud as 'synthetic' sediment to rehabilitate severely eroded marsh areas in Louisiana wetlands showed that approximately 63% of the total Cd, 50% of the total Cu, 13% of the total Ni and 15% of the total Zn was available for partitioning [7].

Several attempts have been made for the effective utilization of raw red mud in many engineering applications. Some of these are: absorbents for sulphur dioxide and hydrogen sulphide in gas purifiers [8]; adsorbents for removal of heavy metal and metalloid ions, inorganic anions such as nitrate and phosphate [8,9]; building materials in the form of aggregates, bricks and cement additive [10,11]; catalysts [12,13]; paints and pigments [14,15]; and recovery of valuable metals [16,17].

Reuse of red mud in the construction materials such as bricks and cement additives have large potential in the developing countries because of high infrastructural development activity. However, the environmental impact of the finished product

* Corresponding author. Present address: Department of Civil and Environmental Engineering, Northeastern University, Boston, MA 02115, USA. Tel.: +1 781 4201817; fax: +1 617 3734419.
E-mail address: ighosh@coe.neu.edu (I. Ghosh).
[1] Deceased.

0304-3894/$ – see front matter © 2010 Elsevier B.V. All rights reserved.
doi:10.1016/j.jhazmat.2010.09.069

obtained from red mud has by and large, remained an uncharted area. To bring about the effective utilization of red mud, such pollution potential of the finished form need to be studied in conjunction with the raw red mud.

Objective of this paper is to compare the leachability of trace metals from fresh red mud and the sintered product which is equivalent to its use as brick and cement additives. In this study, the leaching potential was evaluated on the unit weight basis of the sintered product of pure red mud and this was compared to the leaching potential per unit weight of the raw red mud. This analysis will also provide an estimate of the leaching potential for any product if the proportion of red mud in the composition is known. However, it is to be noted that the mineralogical phase transformation during sintering may be different in different mixture composition and also dependent on temperature and time of sintering.

2. Materials and methods

2.1. Red mud

Red mud samples were collected from the alumina plant of Hindustan Aluminum Company (HINDALCO) at Renukoot, UP, India. Fresh samples were collected in a polyethylene bucket from the hopper of the drum filter used for filtering the red mud slurry. Samples collected over a period of 24 h were transported to the laboratory in sealed polyethylene bags. The red mud samples were clayey in appearance with approximately 70% solid content. For all experiments with fresh red mud, samples were dried in an oven at 108 °C for 24 h, cooled and stored in a desiccator prior to use.

2.2. Sintering of red mud

For sintering, fresh red mud was dried at 108 °C for 24 h, crushed to powder form and stored in the desiccator. Powdered red mud samples with measured water content were cold pressed using a hydraulic press of Construction Ltd., Gravesend, England to form cylindrical pellets of length and diameter 13 mm (approximate). The ram diameter was 65.09 mm and the load used for compaction was 4 metric tons. Sintering was performed at 800 °C in a resistance type vertical tube furnace of diameter 89 mm, length 457 mm and maximum temperature 1000 °C for durations of 1, 2, 3 and 4 days.

2.3. Leaching studies

Leaching tendency of different metals present in red mud, both before and after sintering, was evaluated by sequential extraction procedure [18]. For the leaching experiments with fresh red mud, samples were crushed to powder form, dried in an oven at 108 °C for 24 h, cooled to room temperature and stored in a desiccator. For the leaching experiments with sintered red mud, the pellets sintered at 800 °C were initially broken using an Instron Universal Testing Machine (Model 1195) and crushed into powder form using a mortar and pestle, dried in an oven at 108 °C, cooled and stored in a desiccator. All extraction solutions in each step of the extraction procedure were prepared with deionized water from a Millipore Milli-Q3RO system. The sequential extractions with fresh red mud were carried out in five replicates while the extractions with sintered red mud were carried out in triplicate due to limitation of sample.

For each experiment, 10 g of red mud sample (dry weight, precision 0.1 mg) and a known volume of extract solution were agitated for a fixed duration in a 500 mL glass bottle with ground glass stopper. Volume and the type of the extract solution as well as the degree of agitation varied depending on the step of extraction as outlined below. After each extraction step, the leachate was separated from the residue by filtering through a 0.22 μm Millipore filter paper using a glass Millipore vacuum filter assembly since, 99% of the particles were measured to be larger than 0.2 μm. The leachate was acidified to pH < 2 and stored in a glass bottles for metal analysis. The residue on the filter paper was carried over to the next step of sequential extraction. Different steps of the sequential extraction are as follows [18]:

2.3.1. Exchangeable

The extract solution was 100 mL of 1 M magnesium chloride ($MgCl_2$) of pH 7.0. The bottles were continuously agitated for 24 h in a rotary shaker at room temperature.

2.3.2. Bound to carbonates

The extract solution was 100 mL of 1 M sodium acetate. The pH was adjusted to 5.0 with acetic acid. The bottles were continuously agitated for 24 h in a rotary shaker at room temperature.

2.3.3. Bound to iron oxide

The extract solution was 100 mL of 0.04 M hydroxylamine hydrochloride ($NH_2OH{\cdot}HCl$) in 25% (v/v) acetic acid. Extraction was carried out at 96 + 3 °C for 6 h with occasional agitation on a magnetic stirrer provided with a heater.

2.3.4. Bound to organic matter

This method was adopted from Gupta and Chen [19]. To the residue from the previous step were added 30 mL of 0.02 M HNO_3 and 50 mL of 30% H_2O_2 adjusted to pH 2 with HNO_3, and the mixture was heated to 85 ± 2 °C for 2 h with occasional agitation. A second 30 mL aliquot of 30% H_2O_2 (pH 2 with HNO_3) was then added and the sample was heated again to 85 ± 2 °C for 3 h with intermittent agitation. After cooling, 50 mL of 3.2 M NH_4OAc in 20% HNO_3 (v/v) was added and the sample was diluted to 200 mL followed by continuous agitation for 30 min. The addition of NH_4OAc was designed [19] to prevent adsorption of extracted metals onto the oxidized sediment.

2.4. Total metal by microwave digestion

Total extractable metals in fresh and sintered red mud samples were also analyzed using microwave digestion [20]. Two subsamples, each of 0.5 g (±0.001 g) of fresh or sintered red mud were taken in fluorocarbon polymer microwave vessels. To each of these vessels 9 ± 0.1 mL conc. HNO_3 and 3 ± 0.1 mL 30% H_2O_2 were added. The vessels were sealed according to the manufacturer's direction and were digested in a microwave digester (Model ETHOS E, Milestone, Australia) using the microwave assisted acid digestion method (EPA Method 3051A). The temperature increased to 175 ± 5 °C in approximately 5.5 ± 0.25 min and maintained for 4.5 ± 0.25 min. At the end of the microwave program, the vessels were allowed to cool and the digested samples were filtered through 0.22 μm filter paper using a glass Millipore vacuum filter assembly prior to analysis for metal concentrations.

2.5. SEM–EDS

Scanning electron microscopy and Energy Dispersive Spectroscopy (EDS) based on the principle of Elemental Dispersion Analysis using X-Rays (EDAX) were performed on fresh red mud samples using a scanning electron microscope (SEM) (Model JXA 840, JEOL, Japan), operating at 15 kV accelerating voltage. EDS was performed on a selected area to obtain a surface average composition of the sample.

2.6. X-ray diffraction

In order to identify phase changes occurring in the red mud due to sintering, the X-ray diffraction experiments were carried out on the fresh red mud, sintered red mud, the residues from the microwave digestion and the residues from the sequential extraction. All samples were dried at 108 °C and stored in the desiccator prior to analysis. X-ray diffraction (XRD) measurements were performed in X-Ray Powder Diffractometer Model ISO-Debyeflex 2002, Rich Seifert & Co., Germany, using Cu-K_α with $\lambda = 1.541841$ Å. The scan rate was 3°/min. The diffraction patterns were analyzed using DIFFRAC^{plus} (Release 2001 Eva version 7.0) software from Bruker Advanced X-Ray Solutions, Germany, with the aid of JCPDF database available on the software.

2.7. Mössbauer spectroscopy

Mössbauer spectroscopy was used for studying iron oxides, hydroxides and oxy-hydroxides in fresh and sintered red mud samples as there is no interference in this method [21] due to presence of species of metals other than iron. Mössbauer spectra were recorded in transmission mode using a Mössbauer spectrometer Model Wissel, Germany. Cobalt (Co^{57}) with an activity of 50 millicurie was used as the source. Initial calibration of the spectrometer was carried out by using α-Fe as the standard.

2.8. Metal analysis in the aqueous samples

Metal analyses in the leachate from each of the four steps of sequential extraction and extracts from microwave digestion of fresh and sintered red mud were performed using a Atomic Absorption Spectrophotometer (AAS) of Varian, Inc., USA, Model 220 FS. The metal standards used in analyses were procured from SISCO Research Laboratories Pvt. Ltd, Mumbai, India. The metal concentrations were recorded in mg/L of sample and converted to the unit of mg/kg of dry red mud. Analysis for each sample, standard and blank was done in triplicate. The samples were diluted appropriately using serial dilution whenever needed, to obtain the concentration within the ranges of the standards. The ranges of the standards and the wavelengths of detection for different metals were: Cu 1.0–5.0 mg/L at 324.8 nm; Cr 2.0–10.0 mg/L at 357.9 nm; Pb 5.0–15.0 mg/L at 217 nm; Cd 0.5–2.0 mg/L at 228.8 nm; Fe 2.0–10.0 mg/L at 248.3 nm; Al 20.0–80.0 mg/L at 308.3.

3. Results

In order to assess the bulk elemental composition of the red mud, surface average SEM–EDS was conducted on the fresh red mud samples. The results indicated presence of the following elements in atomic%: aluminum (Al) 15%, silicon (Si) 8.1%, calcium (Ca) 3%, titanium (Ti) 24.5%, vanadium (V) 0.7%, manganese (Mn) 1% and iron (Fe) 47.7%. Sodium was also present but it was not included in the calculations as it was not known to be toxic. Amongst these elements, the WHO guidelines [22] for drinking water exist for Al, Fe and Mn and, therefore are the elements of concern for the leaching studies. Since Mn was present in comparatively smaller amounts in fresh red mud, the main focus was on Al and Fe for the present study. Although the WHO guideline values for the aqueous concentration of Fe and Al in drinking water were quite high, they were present in large proportions in red mud. In addition to these macro-constituents of red mud detected by SEM–EDS, literature indicated the presence of copper (Cu), chromium (Cr), lead (Pb), cadmium (Cd), nickel (Ni) and zinc (Zn) in trace concentrations in red mud [7].

For the extraction and leaching results described in this paper, "total extractability" refers to extractable metal by microwave digestion using EPA Method 3051A and "leachability" refers to the metal concentrations obtained by sequential extraction steps. Nickel and zinc were not detected in any of the fresh or sintered red mud samples that were used in this study either by microwave digestion or by sequential extraction. Cadmium was present in the extracts at very low concentrations in the fresh red mud, but none was detected in the extracts from the sintered red mud (Table 1). Therefore, the leaching results are presented on the following metals: Al, Fe, Cu, Cr and Pb. It was convenient to divide them into two groups and study them separately: macro-elements Al and Fe present in the order of g/kg and, micro-elements Cu, Cr, and Pb present in the order of mg/kg. For the macro-elements, the effect of sintering on leachability could be studied from the mineralogical composition using XRD analysis because they are present in substantial amounts.

Table 1
Total extractable metals in fresh and sintered red mud obtained from extraction by microwave digestion.

Metals	Fresh red mud	Sintered red mud at 800 °C
Aluminum (Al)	131.741 ± 32.595 g/kg	63.355 ± 2.852 g/kg
Iron (Fe)	108.482 ± 4.331 g/kg	15.714 ± 4.872 g/kg
Copper (Cu)	41.3 ± 5.01 mg/kg	26.16 ± 4.13 mg/kg
Chromium (Cr)	395.14 ± 30.20 mg/kg	245.81 ± 27.19 mg/kg
Lead (Pb)	20.224 ± 1.167 mg/kg	32.01 ± 3.757 mg/kg
Cadmium (Cd)	0.037 ± 0.009 mg/kg	ND
Nickel (Ni)	ND	ND
Zinc (Zn)	ND	ND

ND = not detected.

3.1. Effect of sintering on the mineralogical composition of red mud

The minerals of Al and Fe are the primary constituents of red mud. So, it was essential to examine the mineralogy of fresh and sintered red mud through X-ray diffraction in order to understand the extractability of Al and Fe. The phase identified in the fresh red mud with multiple saturation peaks were, hematite (rhombohedral Fe_2O_3-JCPDF 72-0469), anatase (b.c.t. TiO_2-JCPDF 21-1272), gibbsite (monoclinic $Al(OH)_3$)-JCPDF 33-0018), goethite (orthorhombic FeO(OH)-JCPDF 29-0713), calcium silicate hydrate (orthorhombic $Ca_2SiO_4{\cdot}H_2O$-JCPDF 29-0373), calcium aluminum oxide hydrate (b.c.c. $Ca_3Al_2O_6(H_2O)_6$-JCPDF 79-1286), calcium silicate hydroxide (orthorhombic $CaSiO_3(OH)_2$-JCPDF 73-2111), and sodium silicate (orthorhombic $Na_2Si_2O_5$- JCPDF 22-1397). This analysis served as the reference for all the subsequent XRD analyses of sintered samples. As a result of sintering, the peaks belonging to sodium silicate, calcium silicate hydrate, calcium aluminum oxide hydrate and goethite disappeared from the system. Instead, the new peaks appeared and were identified as sodium aluminum silicate (orthorhombic $NaAlSiO_4$-JCPDF 37-0072), calcium aluminum silicate (tetragonal $Ca_3Al_3Si_3O_{12}$-JCPDF 34-1417) and aluminum oxide theta-alumina θ-Al_2O_3 (JCPDF 47-1771). The peaks due to hematite (Fe_2O_3), especially at higher 2θ showed a small shift to the right in the sintered sample while in fresh red mud samples they matched exactly with the database. This may indicate incorporation of other ions in the Fe_2O_3 lattice.

Comparison of isomeric shift (IS) and quadruple splitting (QS) parameters of sextet and doublet in the Mössbauer spectra of fresh (Fig. 1a) and sintered red mud (Fig. 1b) with those of standard confirmed the presence of hematite and goethite in both in both fresh and sintered red mud samples. Conversion of goethite to hematite on sintering was also established by comparing the areas of the peaks in the doublet (goethite) and sextet (hematite) in the Mössbauer spectra before (Fig. 1a) and after sintering (Fig. 1b). Relative proportions of hematite and goethite were estimated approxi-

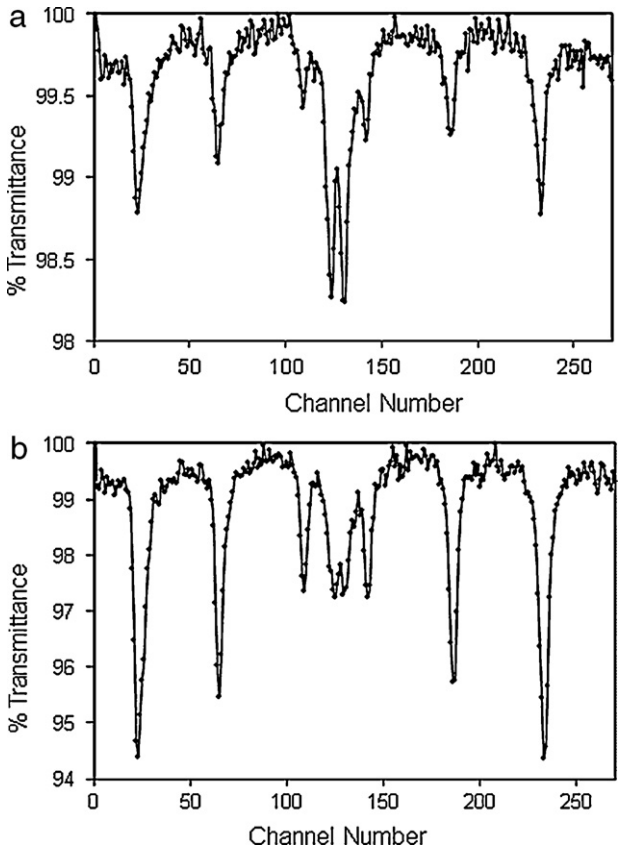

Fig. 1. Comparison of Mössbauer spectrum of red mud before and after sintering (a) fresh red mud and (b) red mud sintered at 800 °C for 4 days.

mately from the sum of the areas of the peaks in sextet and doublet, respectively. The proportions of hematite and goethite in the fresh red mud sample were 61.1% and 38.9%, respectively. The same in the sintered sample were 89.1% and 10.9%, respectively. Sextet in both the samples had a magnetic field of 509.559 kOe, which is lower than that for hematite (519 kOe). This is possible if some other metals are incorporated (doping) in the lattice of hematite. The difference was observed in both fresh and sintered red mud samples indicating that some amount of doping may have been present in both the samples.

3.2. Effect of sintering on total extractability by microwave digestion

The total extractable metals determined by microwave digestion of fresh and sintered red mud (at 800 °C for 4 days) samples are shown in Table 1. Extractability of all the metals with the exception of lead decreased as a result of sintering. The relative amounts of decrease were: Al-51.8%, Fe-85.5%, Cu-36.7% and Cr-37.8%. The extractability of Pb, on the other hand, increased by 81.6% as a result of sintering. All the changes were statistically significant at 95% confidence level when compared using *t*-test.

Comparison of the XRD patterns of fresh red mud and the residue after extraction by microwave digestion of fresh red mud is shown in Fig. 2. Here the peaks, observed in the XRD pattern of fresh red mud, due to gibbsite at '1' and '7', due to goethite at '2' and '5', due to sodium silicate at '3', due to calcium silicate hydrate at '4' and '8', and due to calcium aluminum oxide hydrate at '6' were not present in the XRD pattern of the residue after microwave digestion of fresh red mud. These results clearly showed that the hydrated complexes were extracted in the microwave digestion and were the key contributors to the metal concentrations in the extract. These peaks

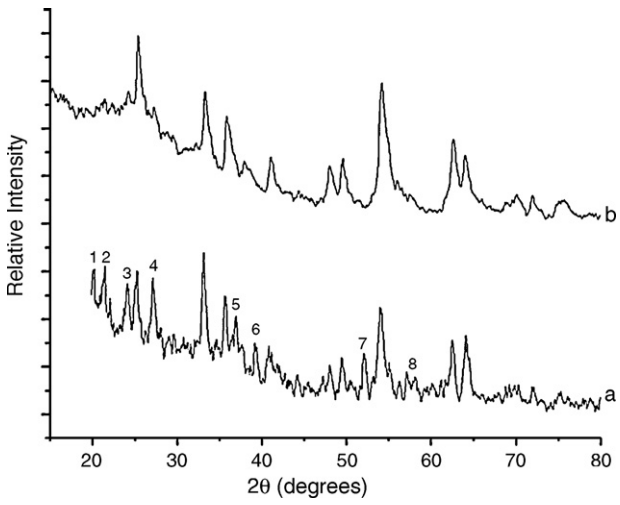

Fig. 2. Comparison of XRD patterns of fresh red mud before and after total extraction of metals by microwave digestion (a) fresh red mud and (b) residue after microwave digestion of fresh red mud. Observed peaks 1, 7: gibbsite $Al(OH)_3$; 2, 5: goethite FeOOH; 3: sodium silicate $Na_2Si_2O_5$; 4, 8: calcium silicate hydrate $Ca_2SiO_4{\cdot}H_2O$; 6: calcium aluminum oxide hydrate $Ca_3Al_2O_6(H_2O)_6$.

were absent in the sintered red mud and the total metal concentrations in the extract decreased. No noticeable differences in the XRD patterns were noticed before and after the extraction by microwave digestion of the sintered red mud (Fig. 3). Small amounts of metal extracted by microwave digestion did not affect the XRD patterns of the stable phases produced by sintering.

3.3. Effect of sintering on leachability by sequential extraction

The amounts of Al and Fe leached out at various steps of sequential extraction of fresh and sintered red mud is shown in Table 2. Total amounts of Al and Fe leaching during sequential extraction was small (~10% for Al and 1% for Fe) compared to the total extractable metals (Table 1). Total leachable Al and Fe due to sequential extraction increased due to sintering. Increase in the leachability of Fe was approximately 3.5 times from 0.149 g/kg in fresh red mud to 0.58 g/kg in sintered red mud and that for Al was approximately 1.5 times from 16.008 to 23.443 g/kg. Major con-

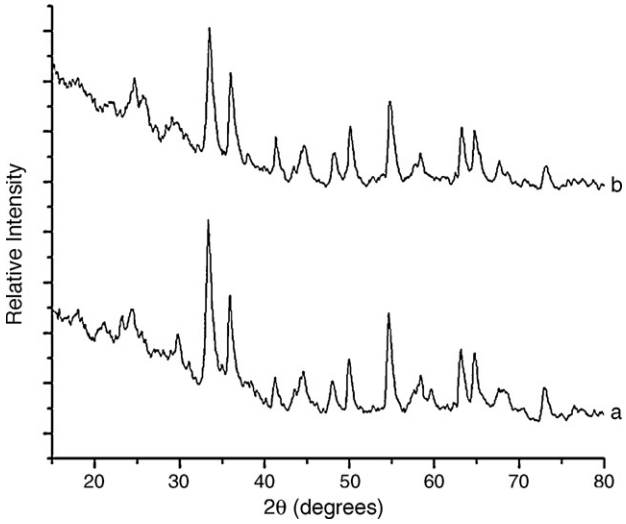

Fig. 3. Comparison of XRD patterns of sintered red mud before and after total extraction of metals by microwave digestion (a) sintered red mud and (b) residue after microwave digestion of sintered red mud.

Table 2
Leachability of macro metals in fresh and sintered red mud at different steps of sequential extraction.

Description	Aluminum (Al) (g/kg)		Iron (Fe) (g/kg)	
	Fresh	Sintered	Fresh	Sintered
Exchangeable fraction	ND	0.154 ± 0.051	ND	ND
Bound to carbonates	8.886 ± 8.153	7.631 ± 0.644	0.003 ± 0.003	0.05 ± 0.004
Bound to iron oxides	3.546 ± 2.202	10.648 ± 5.782	0.138 ± 0.02	0.495 ± 0.696
Bound to organic matter	3.576 ± 4.035	6.836 ± 3.165	0.008 ± 0.013	0.035 ± 0.020
Total leachable	16.008 ± 6.36	23.443 ± 3.566	0.149 ± 0.023	0.58 ± 0.674

ND = not detected.

tributions to the increase in leachability were from the fractions bound to 'iron-oxide' and 'organic matter' (Table 2).

The XRD taken after four steps of sequential extraction of fresh red mud was compared with that of the fresh red mud (Fig. 4). The peak due to calcium aluminum oxide hydrate indicated by '6' in fresh red mud was absent in the residue after sequential extraction. Intensity of the goethite peaks '2' and '5' in fresh red mud decreased slightly to peaks '9' and '12' in the residue. The peaks due to gibbsite indicated by '1' and '7' remained nearly unaltered as indicated by '8' and '13' in the residue. Presence of goethite and gibbsite in the residue indicated that they did not contribute significantly to leaching of the metals in sequential extraction as opposed to total extraction by microwave digestion where these peaks disappeared (Fig. 2). The peaks indicated by '3' and '10' in fresh red mud and residue, respectively could be attributed to either sodium silicate or hematite.

By comparing the patterns of sintered red mud with that of the residue obtained after the sequential extraction of sintered red mud, no significant changes in the phases were noticed (data not shown). Recall that the oxy-hydroxide phases where the changes were noticed for the fresh red mud were already absent in the sintered red mud XRD pattern.

The leachability of the micro-metals in sintered red mud did not follow a uniform pattern (Table 3). After sintering, the total leachability during the sequential extraction decreased for copper (Cu) but increased for chromium (Cr). The leachability of Cu, after sintering, decreased the most in the iron oxide phase. The extractability of Cr, after sintering, increased in all the four leaching fractions, but particularly in the fraction bound to carbonates. Lead (Pb) was not detected in any of the leaching fractions, and therefore non-detect results were not included in Table 3. However, recall that total extraction by microwave digestion of the sintered product contained Pb (Table 1). Therefore, Pb is contained in a phase that is not leachable in any of the procedure described in sequential extraction.

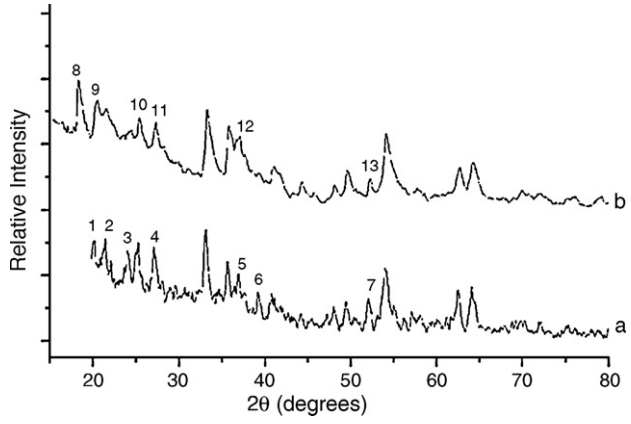

Fig. 4. Comparison of XRD patterns of fresh red mud before and after leaching of metals by four step sequential extraction (a) fresh red mud and (b) residue after sequential extraction of fresh red mud. Observed peaks 1, 7, 8, 13: gibbsite $Al(OH)_3$; 2, 5, 9, 12: goethite FeOOH; 3, 10: sodium silicate $Na_2Si_2O_5$; 4, 11: calcium silicate hydrate $Ca_2SiO_4{\cdot}H_2O$; 6: calcium aluminum oxide hydrate $Ca_3Al_2O_6(H_2O)_6$.

4. Discussion

The leaching of metal during sequential extraction cannot be compared directly with the total extractability by the microwave digestion since these are two independent characterizations of the metals in the red mud. Total extractable metal by microwave digestion decreased due to sintering for all metals (Table 2). The XRD patterns clearly showed that (Fig. 2) the microwave digestion of fresh red mud resulted in the disappearance of the hydroxide and oxy-hydroxide phases. Therefore, predominant contributions of Al and Fe in total extraction of fresh red mud by microwave digestion were from gibbsite, calcium aluminum oxide hydrate and goethite. As a result of sintering at 800 °C, all the hydrated mineral forms of aluminum had disappeared as observed in the XRD patterns and proportion of goethite decreased significantly as was concluded from the Mössbauer spectra (Fig. 1). This would explain the reduction of total extractability of the metals (by microwave digestion) due to sintering.

In contrast, total amounts of Al and Fe leaching out into solution during sequential extraction increased in the sintered sample compared to fresh red mud sample (Table 2). In the sequential extraction, contribution from the hydrated phases was small as the peaks in the XRD patterns corresponding to these phases remained even after extraction from fresh red mud (Fig. 4). As a result, disappearance of these phases due to sintering did not affect the leachability in the sequential extraction much. For aluminum, increases in the 'exchangeable', 'bound to iron oxide' and 'organic matter' fractions were statistically significant while the change in 'bound to carbonate' fraction was not. For iron, increases in the 'bound to iron oxide' and 'organic matter' fractions were statistically significant. Maximum increase for both Al and Fe was noticed in the fraction bound to iron oxide followed by the fraction bound to organic matter. The Mössbauer results showed that proportion of iron oxide (hematite) increased due to sintering (Fig. 1). If some Al was present as co-ordination complex in the lattice of goethite, the conversion to more stable form of hematite would have resulted in the reduction of the amount leached out in the iron oxide fraction. The increase in Al leaching out in the iron oxide fraction indicated that some Al was presumably adsorbed on the goethite phase. The leaching of Fe associated with iron oxide increased with proportion of iron oxide but was limited by the solubility of Fe (III). Due to sintering at 800 °C, it was expected that the organic matter would disappear and the leachability of metals associated with this fraction would increase. Carbonate fraction for Al and Fe did not show significant changes as a result of sintering. The XRD results of raw red mud negated the presence of any significant carbonate mineral. This would indicate that the leachability of small amounts of Al and Fe associated with carbonate were not affected by sintering. Exchangeable fraction of aluminum increased after sintering which presumably was a result of some complexed aluminum ions becoming free as a result of sintering.

Table 3
Leachability of trace metals in fresh and sintered red mud at different steps of sequential extraction.

Description	Copper (Cu) (mg/kg)		Chromium (Cr) (mg/kg)	
	Fresh	Sintered	Fresh	Sintered
Exchangeable fraction	0.83 ± 0.03	0.87 ± 0.03	10.70 ± 1.05	55.12 ± 12.38
Bound to carbonates	2.28 ± 0.98	1.89 ± 0.06	2.74 ± 0.55	109.1 ± 19.93
Bound to iron oxides	7.13 ± 0.72	0.36 ± 0.09	9.78 ± 4.06	26.23 ± 8.14
Bound to organic matter	0.94 ± 0.11	1.41 ± 1.06	12.33 ± 1.99	17.5 ± 2.98
Total leachable	11.18 ± 1.0	4.52 ± 1.22	35.55 ± 6.89	207.95 ± 24.3

The trace metals Cu and Cr are either adsorbed or present as co-ordination complexes in the minerals of Al and Fe. Recall that the magnetic field of the sextets in the Mössbauer spectra indicated that doping in the lattice of hematite was present in both fresh and sintered red mud. Both Cu and Cr showed statistically significant decrease in the total extractability (by microwave digestion) due to sintering (Table 1). However, as a result of sintering, total leachability by sequential extraction increased for Cr while it decreased for Cu Table 3).

There was no statistically significant difference between fresh and sintered red mud in the concentrations of Cu in the exchangeable and 'bound to carbonates' fractions. However, leaching of Cu 'bound to iron oxide' fraction decreased and 'bound to organic' fraction increased significantly as a result of sintering. Copper was presumably associated with the goethite phase in the red mud as a coordination complex bonded to four close oxygen atoms in an approximate octahedral geometry [23]. The nature of Cu complex formation on hematite is similar to that of goethite [24]. The relative amount of hematite (Fe_2O_3) increased on sintering due to the conversion of goethite to hematite. Consequently, after sintering more Cu was associated with the stable Fe_2O_3 phase and thus its leachability in the 'bound to iron oxide' fraction decreased on sintering. At this juncture, recall that leaching of iron in the 'bound to iron oxide' step increased in the sintered sample. Decrease of Cu in the 'bound to iron oxide' phase indicated that incorporation (doping) of Cu in the hematite lattice was non-uniform. The increase in leachability of Cu in the 'bound to organic matter' fraction was the result of loss of organic matter from the red mud on sintering at 800 °C and the subsequent leaching out of Cu that was bound to this organic phase.

Chromium on the other hand leached out to a greater extent in each of the exchangeable, 'bound to carbonates', 'bound to iron oxide' and 'bound to organic matter' fractions of sintered red mud as compared to that in fresh red mud. The increase in leachability of Cr in the exchangeable fraction indicated that some Cr, which was adsorbed on the surface became free as a result of sintering and the rest remained bound to carbonates, iron oxide and organic matter, to be released in subsequent steps. Large increase in the leachability of carbonate fractions showed that a large amount of Cr was associated with carbonates which became available for leaching due to sintering at 800 °C. The fraction bound to organic matter was on the expected line. The increased leachability of Cr associated with the iron oxide fraction after sintering is contrary to the observation of Cu and needs explanation. Chromium exists as Cr(VI) in red mud [25–27], and chromate species are present in goethite in the form of adsorption complexes through strong hydrogen bonding with OH ligands to surface [26,27]. During the phase conversion of goethite to hematite on sintering, these hydroxyl ligands disappeared and the hydrogen bonds were broken resulting in the increased leachability of Cr associated with the iron oxide phase.

In summary, this paper evaluated the pollution potential of red mud and its sintered product under different environmental conditions by studying the leachability of different metals through sequential extraction. Although total extractability by microwave digestion of most of the metals decreased, the leachability of the macro metals in sequential extraction (Fe and Al) increased on sintering. However for the trace metals (Cu and Cr), no such increase due to sintering in the leachability by sequential extraction could be generalized. While Cu leached out to a lesser extent from the iron oxide fraction of sintered red mud as compared to fresh red mud, Cr leached out to a greater extent in each of the exchangeable, 'bound to carbonates', 'bound to iron oxide' and 'bound to organic matter' fractions of sintered red mud as compared to that in fresh red mud.

Acknowledgements

The authors thank Mr. R.P. Shah and Mr. S.N. Gararia of the Alumina Plant at HINDALCO, Renukoot, India for their permission and assistance in sampling in the plant. The technical assistance for sample preparation and testing by Mr. U. Shankar, Mr. S. Pal and Mr. A. Agnihotri of Advanced Centre for Materials Science IIT Kanpur for X-Ray diffraction, particle size distribution and SEM, respectively is gratefully acknowledged.

References

[1] D.J. Cooling, D.J. Glenister, Practical aspects of dry residue disposal, in: E.R. Cutshall (Ed.), Light Metals Proceedings of the 121st TMS Annual Meeting, San Diego, CA, TMS, 1992, pp. 25–31.
[2] A.R. Hind, S.K. Bhargava, S.C. Grocott, The surface chemistry of Bayer process solids: a review, Colloids Surf. A 146 (1999) 359–374.
[3] NOAA, Sediment Quality Guidelines Developed for the National Status and Trends Program, 1999, Retrieved January 3 2010, from NOAA Office of Response and Restoration: http://response.restoration.noaa.gov/book_shelf/121_sedi_qual_guide.pdf.
[4] C. Brunori, C. Cremisini, P. Massanisso, V. Pinto, L. Torricelli, Reuse of a treated red mud bauxite waste: studies on environmental compatibility, J. Hazard. Mater. 117 (2005) 55–63.
[5] S. Tokalioglu, S. Kartal, L. Elci, Determination of heavy metals and their speciation in lake sediments by flame atomic absorption spectrometry after a four-stage sequential extraction procedure, Anal. Chim. Acta 413 (2000) 33–40.
[6] F. Pagnanelli, E. Moscardini, V. Giuliano, L. Toro, Sequential extraction of heavy metals in river sediments of an abandoned pyrite mining area: pollution detection and affinity series, Environ. Pollut. 132 (2004) 189–201.
[7] G.L. Goldstein, R. Reimers, Trace element partitioning and bioavailability in red mud synthetic freshwater sediment, in: E. Eckert (Ed.), Light Metals 1999 Proceedings of the Technical Sessions Presented by the TMS Aluminum Committee at the 128th TMS Annual Meeting, San Diego, CA, TMS, 1999, pp. 19–24.
[8] S.B. Wang, H.M. Ang, M.O. Tade, Novel applications of red mud as coagulant, adsorbent and catalyst for environmentally benign processes, Chemosphere 72 (2008) 1621–1635.
[9] V.K Gupta, M. Gupta, S. Sharma, Process development for the removal of lead and chromium from aqueous solutions using red mud—an aluminium industry waste, Water Res. 35 (2001) 1125–1134.
[10] T. Kavas, Use of boron waste as a fluxing agent in production of red mud brick, Build. Environ. 41 (2006) 1779–1783.
[11] W.C. Liu, J.K. Yang, B. Xiao, Application of Bayer red mud for iron recovery and building material production from alumosilicate residues, J. Hazard. Mater. 161 (2009) 474–478.
[12] S. Ordonez, H. Sastre, F.V. Diez, Catalytic hydrodechlorination of tetrachloroethylene over red mud, J. Hazard. Mater. 81 (2001) 103–114.
[13] J.R. Paredes, S. Ordonez, A. Vega, F.V. Diez, Catalytic combustion of methane over red mud-based catalysts, Appl. Catal. B: Environ. 47 (2004) 37–45.
[14] J. Pera, R. Boumaza, J. Ambroise, Development of a pozzolanic figment from red mud, Cem. Concr. Res. 27 (1997) 1513–1522.
[15] A. Collazo, D. Fernandez, M. Izquierdo, X.R. Novoa, C. Perez, Evaluation of red mud as surface treatment for carbon steel prior painting, Prog. Org. Coat. 52 (2005) 351–358.
[16] L.V. Tsakanika, M.T. Ochsenkuhn-Petropoulou, L.N. Mendrinos, Investigation of the separation of scandium and rare earth elements from red mud by use of reversed-phase HPLC, Anal. Bioanal. Chem. 379 (2004) 796–802.

[17] Y. Cengeloglu, E. Kir, M. Ersoz, T. Buyukerkek, S. Gezgin, Recovery and concentration of metals from red mud by Donnan dialysis, Colloids Surf. A 223 (2003) 95–101.
[18] A. Tessier, P.G. Campbell, M. Bisson, Sequential extraction procedure for the speciation of particulate trace metals, J. Anal. Chem. 51 (1979) 844–850.
[19] S.K. Gupta, K.Y. Chen, Partitioning of trace metals in selective chemical fractions of nearshore sediments, Environ. Lett. 10 (1975) 129–158.
[20] USEPA, 3051A Method: Microwave Assisted Acid Digestion of Sediments, Sludges, Soils, and Oils, Revision 1, 2007, Retrieved January 3 2010, from USEPA SW-846 Manual: http://www.epa.gov/waste/hazard/testmethods/sw846/pdfs/3051a.pdf.
[21] G.K. Wertheim, Mössbauer Effect: Principles and Applications, Academic Press, New York, 1964.
[22] WHO, Guidelines for Drinking-Water Quality Third Edition Incorporating the First and Second Addenda Volume 1 Recommendations, 2008, Retrieved January 3 2010, from World Health Organization Water Sanitation and Health: http://www.who.int/water_sanitation_health/dwq/GDW8rev1and2.pdf, accessed 3 January 2010.
[23] R.H. Parkman, J.M. Charnock, N.D. Bryan, F.R. Livens, D.J. Vaughan, Reactions of copper and cadmium ions in aqueous solution with goethite, lepidocrocite, mackinawite, and pyrite, Am. Mineral. 84 (1999) 407–419.
[24] J.H. Jung, Y.H. Cho, P. Hahn, Comparative study of Cu^{2+} adsorption on goethite, hematite and kaolinite: mechanistic modeling approach, B, Kor. Chem. Soc. 19 (1998) 324–327.
[25] S. Fendorf, M.J. Eick, P. Grossl, D.L. Sparks, Arsenate and chromate retention mechanisms on goethite. 1. Surface structure, Environ. Sci. Technol. 31 (1997) 315–320.
[26] P.R. Grossl, M. Eick, D.L. Sparks, S. Goldberg, C.C. Ainsworth, Arsenate and chromate retention mechanisms on goethite. 2. Kinetic evaluation using a pressure-jump relaxation technique, Environ. Sci. Technol. 31 (1997) 321–326.
[27] S.X. Yin, D.E. Ellis, DFF studies of Cr(VI) complex adsorption on hydroxylated hematite (1(1)over-bar02) surfaces, Surf. Sci. 603 (2009) 736–746.